Multilabel Leukemia classification machine

Section 3 DATASCI 281 Computer Vision

Dylan Jin, Fabian Riquelme, Luc Robitaille, Dmitri Zadvornov

1. Introduction **2**
2. Hypothesis **2**
3. Literature Review **2**
4. Dataset Description **3**
5. Methodology **4**
5.1 Traditional classification approach 4
5.1.1 Traditional classification approach pipeline 4
5.1.2 Pre-processing activities 5
5.1.2 Segmentation 6
5.1.3 Feature selection 7
5.1.4 Feature extraction 7
5.1.5 Classification with SVM 8
5.2 Our Deep Neural Network Approach to ALL Classification 9
5.2.1 DNN approach overview 9
5.2.2 DNN Pipeline and Architecture 10
5.2.3 Explainability of CNN results 12
6. Results **12**
6.1 SVM Model Results 12
6.2 DNN Model Results 13
7. Conclusions **14**
8. Future work and limitations **15**
8.1 Limitations 15
8.2 Next steps 15
9. References **17**

GitHub Repository: https://github.com/Fnriquel/281-Project

1. Introduction

Leukemia blood cancers account for many annual diagnoses in the United States, with an estimated 60,000 cases identified annually (Leukemia and Lymphoma Society, 2021). One prevalent method for diagnosing Leukemia is the peripheral blood smear, which is minimally invasive and only requires a blood draw. However, preparing and classifying these smears demands the expertise of trained lab technicians and medical professionals (American Cancer Society, 2018). Early cancer detection is crucial for successful treatment, as cancers identified in their initial stages are more likely to be treatable (He et al., 2022).

Automation in the diagnostic process has the potential to reduce costs and increase testing frequency, leading to higher sampling rates and, consequently, improving the likelihood of early detection and survival rates for the Leukemia family of cancers. In this paper, we present a project to perform multilabel classification on Acute Lymphoblastic Leukemia (ALL) peripheral blood smear data to classify ALL and the stage present in the sample. Additionally, we investigate the effectiveness of manually extracted features with traditional Machine Learning models (e.g., Support Vector Machines) compared to more advanced Deep Learning techniques, particularly in cases where labeled data is limited.

2. Hypothesis

Given a limited dataset size, we hypothesize that standard feature-extraction-based approaches would produce superior outcomes since models based on CNN extraction require a considerable amount of data to be fully trained. For our CNN-based model, we have employed the state-of-the-art (SOTA) EfficientNet-V2L. In addition, our feature extraction involves three traditional methods: Canny Edge Detection, Histogram of Gradients (HoG), and Color basis transformation (LAB and YCbCr). Features will be implemented in traditional Machine Learning classification models: SVM. In both methods, we will obtain multilabel classifications, with the primary metrics being accuracy, F1, and AUC scores.

3. Literature Review

Analyzing recent research, we found that model performance is driven, among other things, by the feature extraction method, feature filtering (reduction) method, and classification model selection (He et al., 2022). Traditional SVM-based methods can achieve reasonably high accuracy scores, with an accuracy of around 96% and an F1 score of 96.22% (Sahlol et al., 2020). This forms the baseline for our SVM performance.

Currently, the highest-performing CNN models for image classification are based on a novel, more efficient approach called EfficientNet. EfficientNet has greater classification accuracy than other CNN models while requiring fewer parameters. Researchers using EfficientNet-B3 on the dynamic classification of Leukemia cells resulted in an accuracy score of 97.57% and an F1-score of 98.22% (Abd El-Ghany, 2023), EfficiantNetV2, from the same family, is currently the highest-performing pre-trained CNN model and up to 6.8 times smaller. One of the key innovations in EfficientNetV2 is using adaptive dropout and data augmentation during training to achieve both fast training and good accuracy, which forms the baseline CNN performance for our study. (Mingxing Tan et al., 2021).

Typical feature extraction methods focus on traits such as color, shape, and texture (Hegde et al., 2020). Some works also include statistical features such as skewness, variance, or gradient

matrix (Patel et al., 2015). More recently, CNN-based extraction methods are gaining popularity, such as AlexNet, CaffeNet, and VGG-f, among others (Vogado et al., 2018). Feature filtering methods include PCA (Das et al., 2020), LDA, and SESSA.

The classification includes traditional methods like DT, SVM, KNN, and DL transfer learning methods based on the models such as VGG, EfficientNet, InceptionNet, and others.

4. Dataset Description

For this project, we will use a dataset containing 3256 peripheral blood smear images from 89 patients suspected of ALL stained by laboratory staff with cytochemical dyes. Each image is split into ALL subtypes and benign cells. The dataset comprises 504 images of healthy cells with benign diagnosis, 985 images of Early Pre-B cells, 963 images of Pre-B cells, and 804 images of Pro-B malignant lymphoblasts. Classification of cell types and subtypes was performed by a specialist using flow cytometry instrumentation.

Each Raw image is RGB formatted with 224 x 224 pixels. The images were taken with the same Zeiss camera on a microscope with 100x magnification and saved as a JPG file. Each image contains one or more stained lymphocyte cells. The cytoplasm of lymphocytes reacts with a light blue color and the nucleus with a deep blue-violet color (Figure 1).

Link to dataset: https://www.kaggle.com/datasets/mehradaria/leukemia

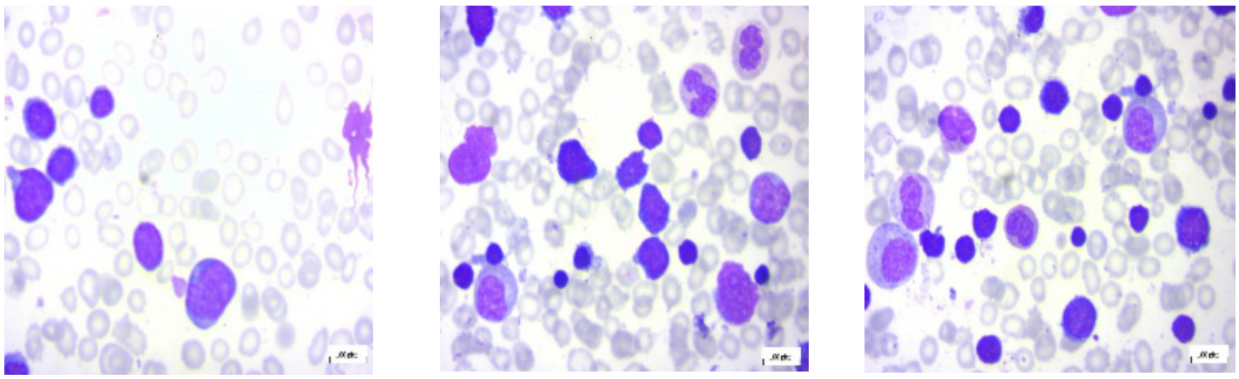

Figure 1: Sample data

The dataset was divided into 80% Training, 10% Validation, and 10% Test.

The dataset comprises images with different brightness and contrast levels, which can affect the accuracy of a convolutional neural network (CNN) when trained. Brightness and contrast are fundamental visual properties of an image, where brightness refers to the overall lightness or darkness of an image, and contrast is the difference between the light and dark regions. Color is another critical characteristic of an image, defined by the presence of hue, saturation, and value. By calculating the mean and standard deviation of each color channel for the images, we can get insights into the distribution of brightness, contrast, and color and determine if there is any variation across the dataset (Figure 2).

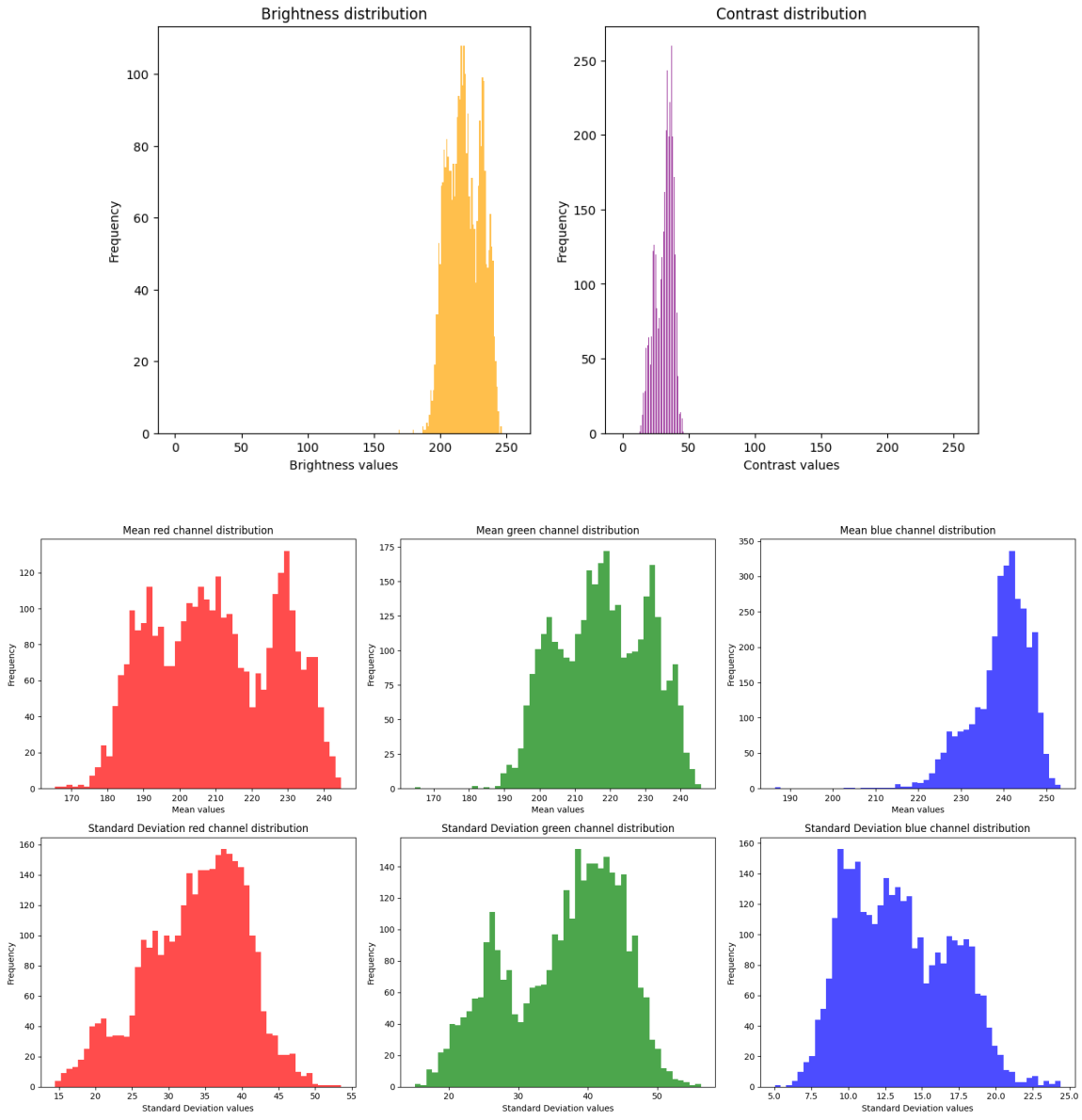

Figure 2: Sample images brightness, contrast, and color channel distributions.

5. Methodology

5.1 Traditional classification approach

5.1.1 Traditional classification approach pipeline

We made a standard pipeline to implement the traditional approach to ALL classification (Saleem et al., 2022). This pipeline includes pre-processing - image enhancement and denoising; segmentation - K-means clustering, thresholding, and morphology; feature extraction - geometry/shape, color, and texture; feature selection - based on information gain, and classification - Support Vector Machine (SVM) (Figure 3).

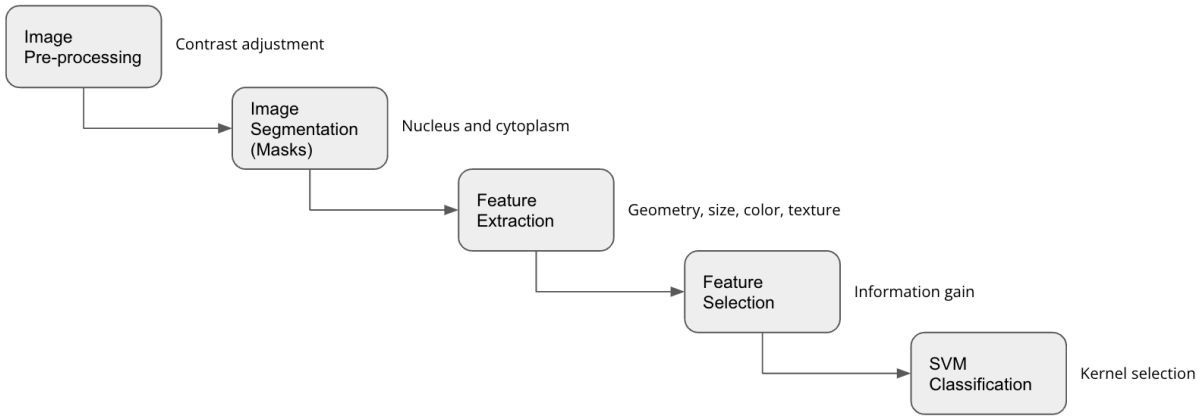

Figure 3: Traditional modeling pipeline

5.1.2 Pre-processing activities

Color Adjustment: The process performs color normalization between the source and template images using the method described by Zhang et al. (2014). The function aims to adjust the source image's color distribution to match manually selected template image's color distribution, resulting in a new color-adjusted image.

Noise Reduction: The process replaces each pixel value with the median value of its neighboring pixels in a given kernel or window, effectively smoothing out the image while preserving the edges and details. In application, the **cv.medianBlur()** function was used with a kernel size of 3.

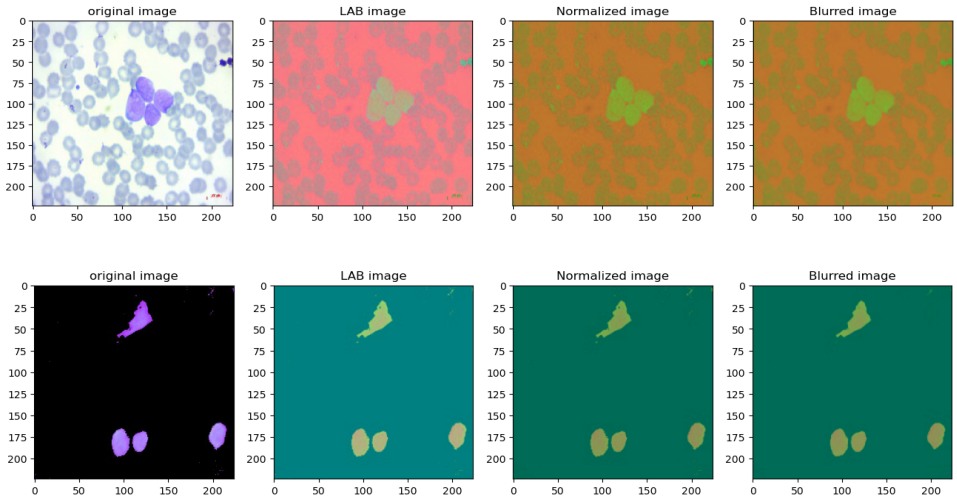

Figure 4: Image Pre-Processing

5.1.2 Segmentation

In the traditional ALL classification approach, segmentation is one of the critical steps, as calculation of most of the features is done with respect to the nucleus or cytoplasm of the white blood cells (WBC), such as nucleus to cytoplasm area ratio, effective diameter, cell count, and other. There are many different approaches to segmentation, with K-means unsupervised classification over the alternative color spaces (e.g., HSV, LAB) among the most successful ones (Saleem et al., 2022).

We take the approach of K-means segmentation over (a,b) features of LAB space of the images with thresholding, morphology operations, and modified watershed segmentation, which previously proved effective (Acharya & Kumar, 2019). First, we segment the WBC nucleus. We apply K-means clustering to (a,b) channels of LAB color space with N=4 to account for the nucleus, cytoplasm, red cells, and background. The nucleus cluster would be the one with the lowest red intensity, and the cytoplasm with the second lowest intensity in red. We then convert the image to binary with a threshold of 0.1 (Acharya & Kumar, 2019). Small particles in the image are removed by applying an area opening with the size of 100 for foreground items and the size of 15 for the background items to fill the holes. The selected objects touching the border are removed with the clear border operation to ensure that partial cells spanning the image border do not affect classification accuracy. The segmentation process is concluded by applying modified watershed segmentation, where minor local minima are filtered out. The distance transform is updated to ensure the local minima do not occur in these locations (Eddins, 2013).

We segment cytoplasm by further segmenting cytoplasm clustering obtained from the first application of K-means, this time with N=3 to account for remnants of red cells, background bleed-over, and cytoplasm. Extracted cytoplasm clustering is converted to a binary image by applying adaptive histogram equalization and Otsu thresholding. Beyond that, we follow the morphology and watershed segmentation steps described above. The resulting process is depicted in Figure 5.

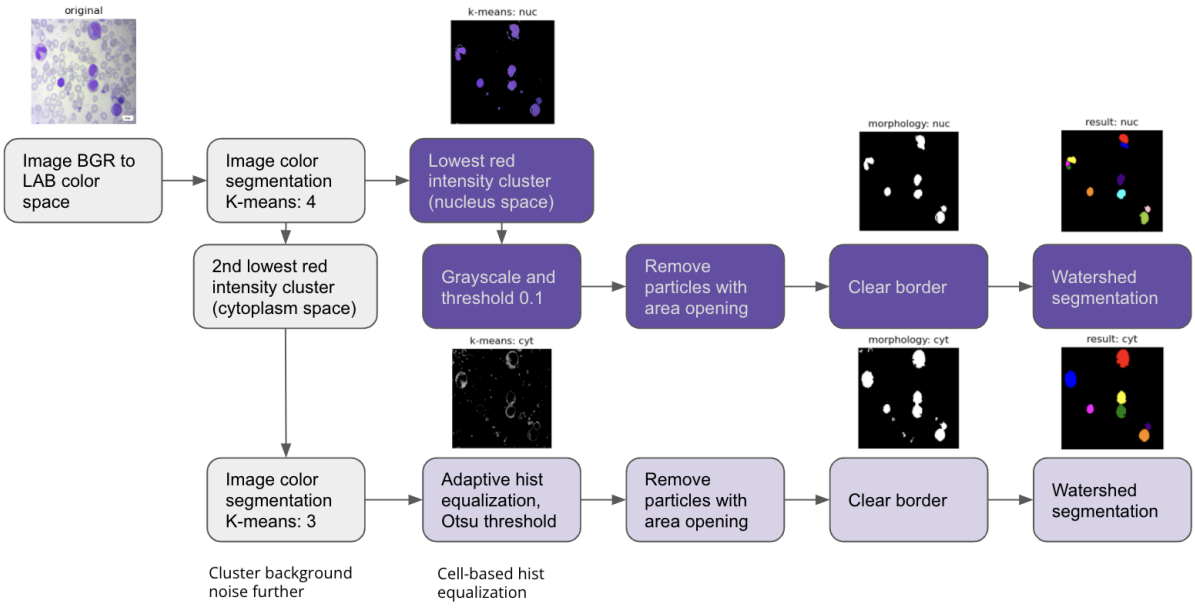

Figure 5: White blood cell segmentation process

5.1.3 Feature selection

During the literature review, several dominant features were identified that are common ALL indicators. These features can be summarized in three subsets: Geometric, Texture, and Statistical features. Geometric features highly correlated with ALL are white blood cell diameter and the white blood cell nucleus diameter ratio to cytoplasm diameter, called the N/C ratio. We use as a guide the list of features evaluated and ranked using information gained per attribute in previous work (Acharya V, Kumar P., 2019). Texture features comprise differences in gradients inside of a single cell, to estimate this we use openCV contour detection and compute Histogram of Gradients (HOG) over the area of the contour identified. Features taken from the HOG are cell max gradient, mean gradient, gradient standard deviation, and percentage pixels with active gradient. Statistical features comprise representative distribution metrics, including mean and standard deviation for the color channel, transformations of color channel basis, and texture features such as Histogram of Gradients.

5.1.4 Feature extraction

Feature extraction was implemented as an iterative process across both segmented and unsegmented images to maintain the separability of the information lost from the segmentation of images.

Geometric Features: Starting with the cornerstones of past research, the geometric features of images were extracted using a combination of Canny edge detection and openCV **findContours()**, which extracts closed-form contours from images as seen in Figure 6. Ultimately, the sum, standard deviation, and mean area of contours in an image were extracted as features.

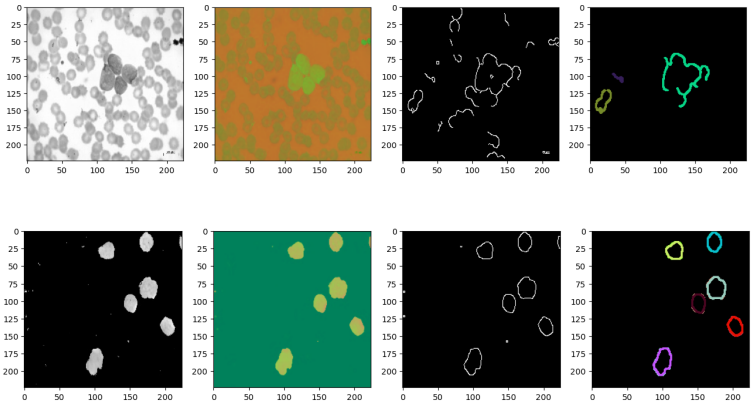

Figure 6: Feature extraction of Cell Contours, Segmented vs Unsegmented Images

Texture Features: Starting with the cornerstones of past research, the texture features of images were extracted using a combination of Canny edge detection and openCV **findContours()**, HoughCircles() which extracts texture information from images as seen in Figure 7. Ultimately, the sum, standard deviation, and mean area of contours in an image were extracted as features.

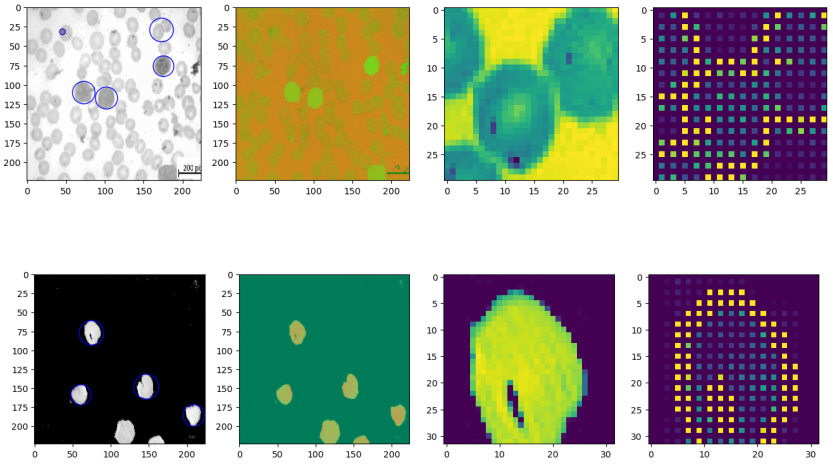

Figure 7: Feature extraction of Cell Texture, Segmented vs Unsegmented Methods

Statistical features: were extracted as summary statistics for the individual distributions, e.g., mean and standard deviation. These summary statistics were extracted from each image and then cast to the distribution of the entire dataset. In Figure 7, readers can see an example of the summary statistics distributions for the LAB color channels.

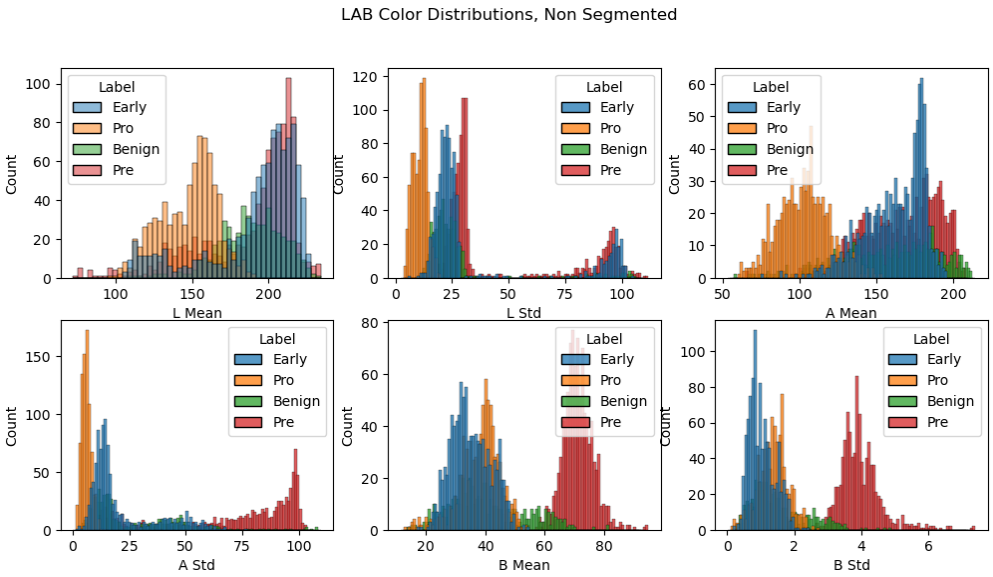

Figure 8: Summary Statistics Distribution by Class, LAB Color Basis

5.1.5 Classification with SVM

Support Vector Machines was selected as the classification technique using manual feature generation. SVMs were selected because of their efficiency, efficacy in high-dimensional spaces, explainability, and common use in Leukemia classification papers. In this application, multiclass SVMs were implemented, and the instantiation variables: kernels and C-values were experimented with to achieve the highest possible classification parameters. The SVM kernel is

a matrix applied to an SVM to create non-linear characteristics in the classifier hyperplane. SVM libraries have an optimized set of kernels for classification applications. Research of similar studies concerning ALL classification supports that the Radial Basis Function kernel, 'RBF,' yielded the best results (Amin et al. I, 2015). The C-Value is a 'slack-variable' cost function to parametrize the classification hyper-plane cost for misclassifying an element. Low C-values are associated with a "Hard-SVM," with a harsh penalty for a reduced margin between the hyperplane and classification elements. High C-values are associated with a "Soft-SVM," with a low penalty for a reduced margin between the hyperplane and classification elements. The trade-off here is in overfitting. If the classes are separable, then the SVM will find the optimal plane to maximize the margin between classification groups at the cost of not generalizing to new data. This application tested feature subsets on various SVM kernel and C-value combinations to find an optimal classifier for the input features.

5.2 Our Deep Neural Network Approach to ALL Classification

5.2.1 DNN approach overview

In recent years, Deep Neural Networks (DNNs) have been state-of-the-art technology for computer vision (El-Ghany et al., 2022). They are the most utilized method for analyzing medical images, classifying, and detecting specific features. In this study, we use this method as the benchmark as it is state of the art and has shown excellent accuracy on a similar task.

Deep neural networks achieve the best results on large data sets, requiring specially designed architectures and sizeable computational power to train a CNN (Sahlol et al., 2020). Due to the magnitude of this task, we have found other methods, such as transfer learning, that can help us leverage DNNs within the resources and time constraints of this project.

Based on the literature review, EfficiantNetV2 is currently the highest-performing pre-trained CNN model, up to 6.8 times smaller. One of the key innovations in EfficientNetV2 is using adaptive dropout and data augmentation during training to achieve both fast training and good accuracy. Figure 8 shows the relative performance of members of the EfficientNet family, as well as other models such as ResNet, Vision Transformer (ViT), and Data-Efficient Image Transformers (DeiT) (Mingxing Tan et al., 2021). Based on those results, we used EfficientNet V2L, which had the best tradeoff between accuracy and training time.

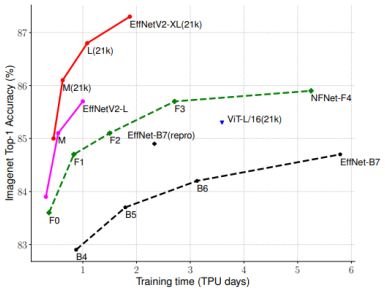

(a) Training efficiency.

	EfficientNet (2019)	ResNet-RS (2021)	DeiT/ViT (2021)	EfficientNetV2 (ours)
Top-1 Acc.	84.3%	84.0%	83.1%	83.9%
Parameters	43M	164M	86M	24M

(b) Parameter efficiency.

Figure 9: Performance of Pre-trained Models

5.2.2 DNN Pipeline and Architecture

Our pipeline for DNN consists of four main stages:

1. Pre-processing: Data balancing between the four classes (Benign, Early, Pre, Pro) and splitting the dataset (60% Training, 20% Validation, 20% Test).
2. Model Creation: Our DNN model comprises an input layer, the EfficentNetV2L functional layer, max pooling/dropout layers to reduce overfitting, and the dense output layer for classification (Figure 9).
3. Model Training: After tuning, we got optimal results with the following hyperparameters:
   Accuracy: Categorical Accuracy
   Optimizer: Adamax
   Batch Size: 25
   Learning Rate: 0.0001
   Training Epochs: 10.

4. Model Testing: Predict the classifications of the test dataset.

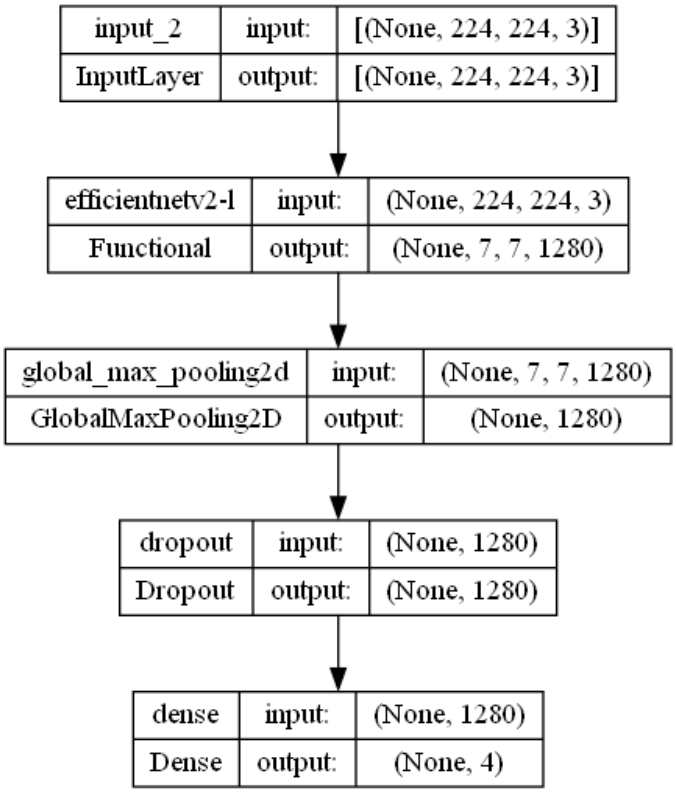

Figure 10: DNN Model Architecture

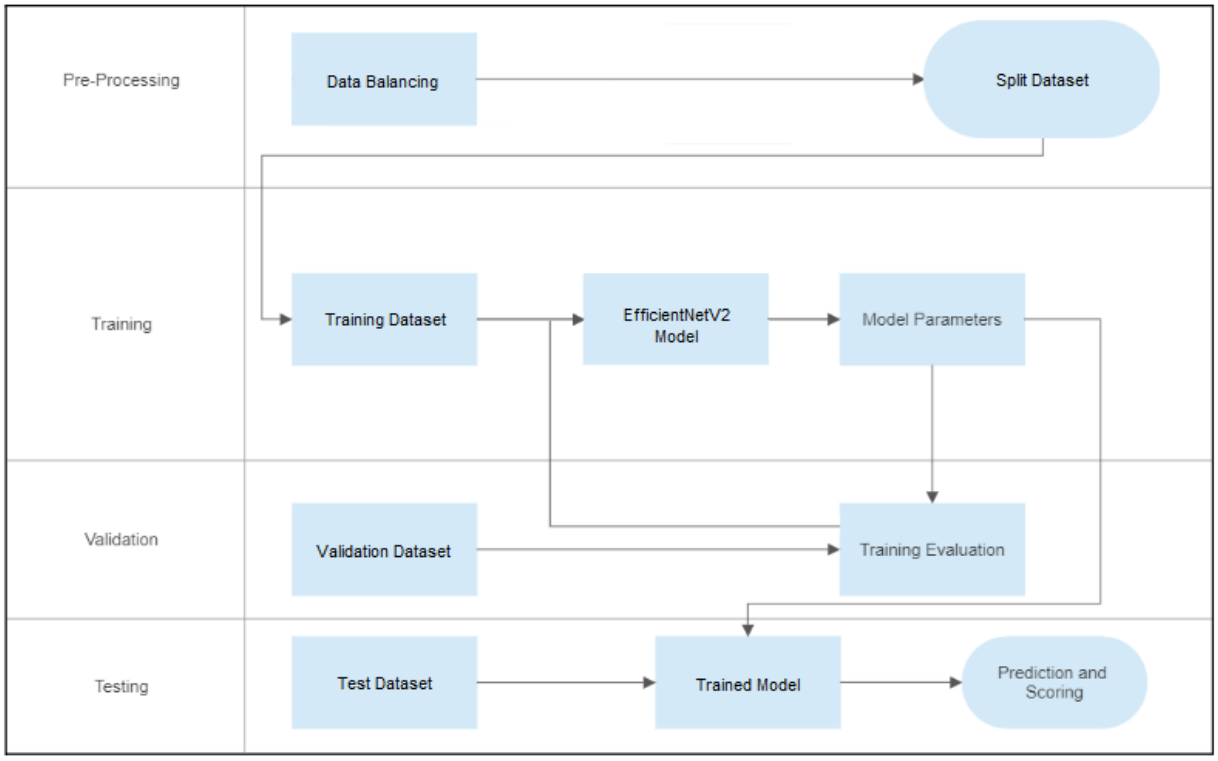

Figure 11: General CNN Pipeline

The pipeline workflow is outlined in Figure 10.

We initially tried to preserve as much of our dataset as possible using data augmentation. However, this led to overfitting (Figure 11). The cause of this overfitting was likely artifacts due to the data augmentation process (Figure 12). Therefore, we decided to balance the dataset based on the smallest subset, eliminating the need for data augmentation. The final dataset used for the DNN approach consisted of 500 images in each of the four categories, for a total of 2000 images. Runs were made with both an 80-10-10 distribution and a 60-20-20 distribution.

Our EfficientNet model was run on the original dataset and the segmented nuclei.

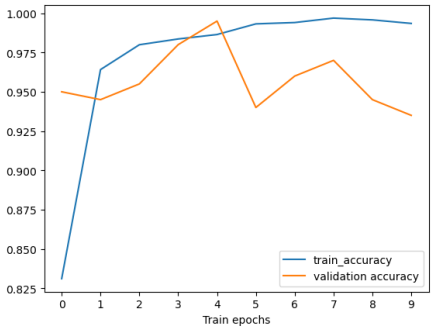

Figure 12: Validation and Training Accuracy Plot

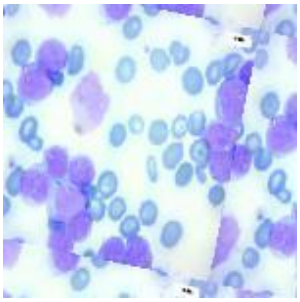
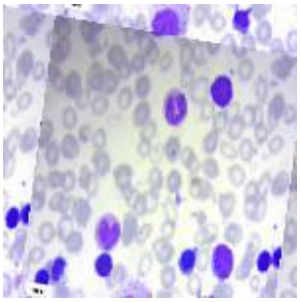

Figure 13: Artifacts on Images

5.2.3 Explainability of CNN results

Gradient-weighted Class Activation Mapping (Grad-CAM), is a widely-used technique in deep learning that facilitates understanding of the image regions a neural network relies on for making predictions. This approach offers valuable insights into the decision-making process of complex models, such as CNNs (Zhou et al., 2016). A key advantage of Grad-CAM is its capacity to deliver visual explanations for the choices made by the neural network, enabling researchers to interpret the model's behavior and make necessary adjustments (Selvaraju et al., 2017). Moreover, by pinpointing the image regions that the neural network utilizes, it becomes feasible to identify parts of the image that are crucial for accurate predictions, subsequently enhancing the model's performance (Chattopadhay et al., 2018).

As explainability is the major concern for adopting the models in a working setting, we utilized the Grad-CAM method to highlight the regions that contributed to the model classification decision and analyze if it aligns with traditional approaches.

6. Results

6.1 SVM Model Results

In this study, several variations of SVM classifiers were evaluated. When applied it on non-segmented images, the model did not perform well, with an accuracy of 56.5%, slightly better than random chance. By incorporating geometric features, Histogram of Oriented Gradients (HoG), a Radial Basis Function (RBF) kernel, and setting the regularization parameter (C) to 96, the model's performance was significantly enhanced, resulting in an accuracy of 82% and an F1 score of 84%. The results of the selected model are in line with the research that utilized traditional features and SVM for classification. However, these results departed from the best SVM-based scores (Saleem et al., 2022) due to higher variations in image quality and additional errors introduced in the segmentation phase.

Models	Accuracy	F1	AUC
Non-segmented SVM (RBF 10)	0.68	0.70	0.907
Non-segmented SVM (RBF 96)	0.82	0.84	0.948

Models	Accuracy	F1	AUC
Segmented SVM (RBF 10)	0.66	0.68	0.910
Segmented SVM (RBF 96)	0.75	0.75	0.940

Figure 13: SVM Model Results

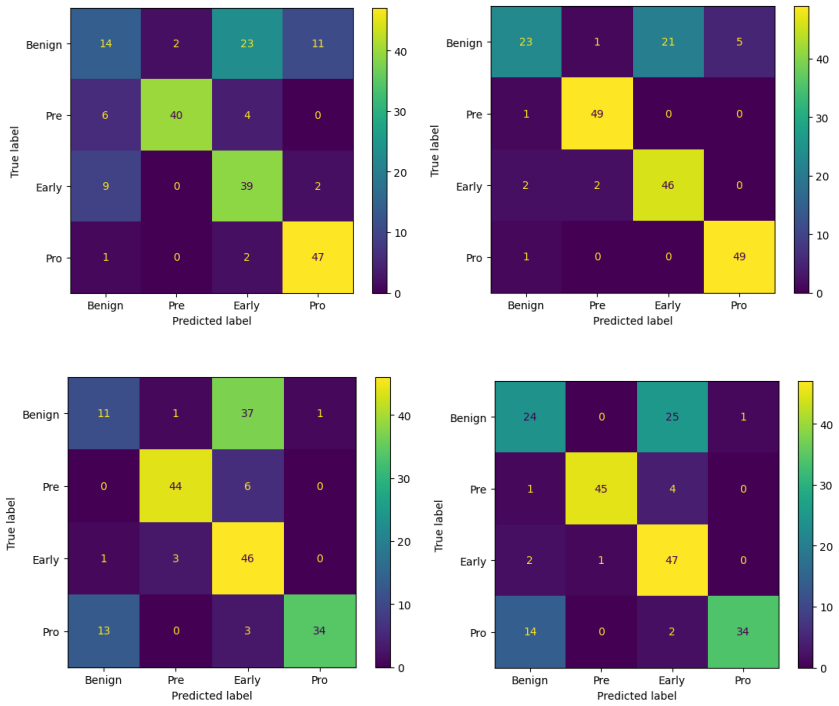

Figure 14: SVM Model Confusion Matrices (Top Left: Non-Segmented (RBF, 10), Top Right: Non-Segmented (RBF, 128), Bottom Left: Segmented (RBF, 10), Bottom Right: Segmented (RBF, 96))

We used the results obtained from the SVM model as a foundation for comparing it with the latest deep neural network (DNN) method, which will be detailed in the following section of this research.

6.2 DNN Model Results

Our initial run from the unsegmented images in the 80-10-10 distribution yielded an unrealistic 100% accuracy when classifying the Pre and Pro classes (Figure 14). This suggested that there were insufficient samples in the Test class, which led us to rerun all of our experiments with a 60-20-20 distribution, which produced more reliable results.

The distribution did not impact the accuracy and F1 scores of the segmented images, which indicates that segmenting the images removed whatever bias was present that made the unsegmented image results unreliable in the 80-10-10 run. However, the segmented images' overall accuracy and F1 scores were about 3% lower than the unsegmented images.

This would suggest that analyzing the white blood cells alone generally provides a good indicator of the stage of leukemia. However, information outside the white blood cells, such as

the morphology and quantity of red blood cells present, is needed for more accurate classification.

Pre-Process	Distribution: 80-10-10	Distribution: 60-20-20
Original		

	precision	recall	f1-score	support
Benign	1.0000	0.9600	0.9796	50
Early	0.9615	1.0000	0.9804	50
Pre	1.0000	1.0000	1.0000	50
Pro	1.0000	1.0000	1.0000	50
accuracy			0.9900	200
macro avg	0.9904	0.9900	0.9900	200
weighted avg	0.9904	0.9900	0.9900	200

	precision	recall	f1-score	support
Benign	1.0000	0.9700	0.9848	100
Early	0.9524	1.0000	0.9756	100
Pre	1.0000	0.9100	0.9529	100
Pro	0.9346	1.0000	0.9662	100
accuracy			0.9700	400
macro avg	0.9717	0.9700	0.9699	400
weighted avg	0.9717	0.9700	0.9699	400

Segmented		

	precision	recall	f1-score	support
Benign	0.8545	0.9400	0.8952	50
Early	0.9592	0.9400	0.9495	50
Pre	0.9434	1.0000	0.9709	50
Pro	1.0000	0.8600	0.9247	50
accuracy			0.9350	200
macro avg	0.9393	0.9350	0.9351	200
weighted avg	0.9393	0.9350	0.9351	200

	precision	recall	f1-score	support
Benign	0.8899	0.9700	0.9282	100
Early	0.9684	0.9200	0.9436	100
Pre	0.9159	0.9800	0.9469	100
Pro	1.0000	0.8900	0.9418	100
accuracy			0.9400	400
macro avg	0.9436	0.9400	0.9401	400
weighted avg	0.9436	0.9400	0.9401	400

Figure 15: DNN Model Results

This was verified from the Grad-CAM images (Figure 15), which visualized areas with the highest weights used by the model to determine the features the model considered important. As expected, we can see the highlights on the nuclei, but the gaps with low red blood cell density were also significant.

Overall, our EfficientNet results align with the baseline results from our literature review, with an overall accuracy score of 97.00% and an F1 score of 96.89%. Given that our dataset was relatively small and our Benign cell classification results exceeded the baseline, the results met our expectations.

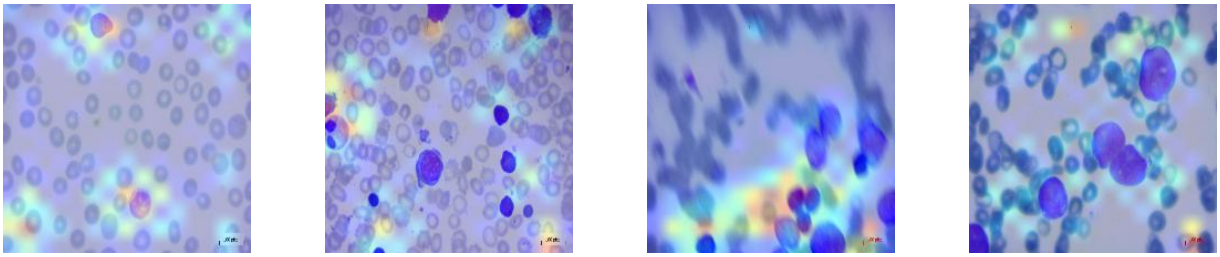

Figure 16: Grad-CAM heatmaps for Bening, Early, Pre and Post Cancer Images

7. Conclusions

Our study highlights the prominence of Convolutional Neural Networks (CNNs) as

state-of-the-art in image classification, particularly in the context of a cancer diagnosis. We observed that the critical regions identified by CNNs correlated with those determined by Support Vector Machines (SVM), indicating synergy between the two approaches. While SVM demonstrated high accuracy in classifying cancerous cells, it could have been more effective in identifying non-cancerous cells.

The EfficientNet-V2L model demonstrated exceptional performance, achieving a 97% accuracy rate, which exceeded SVM's results in classifying cancerous cells. The EfficientNet-V2L model consistently outperformed manually extracted features and the use of SVM. Furthermore, preprocessing techniques were not required to achieve 97% accuracy on the EfficientNet-V2L model. This highlights the potential advantages of using CNNs, such as EfficientNet-V2L, in the field of Cancer diagnosis.

Our experimentation with segmented images yielded inferior results to the original images in both methods used, implying that crucial information may be lost during segmentation. Our work has the potential to uncover features and areas of interest that could assist doctors with diagnosing and staging leukemia in the future. Furthermore, our investigation revealed that using pre-trained models helped mitigate the necessity for extensive datasets, thereby streamlining the development and deployment of effective cancer classification models.

8. Future work and limitations

Despite the promising results and insights gained from this study, certain limitations and areas for future work should be addressed.

8.1 Limitations

- Our study was conducted using a limited dataset, which may not fully capture the variability and complexity of real-world scenarios. Consequently, the generalizability of our results may be restricted.

- The results of the 80-10-10 distribution vs. 60-20-20 indicate some bias or lack of diversity in our dataset.

- The SVM's inability to accurately classify non-cancerous cells indicates the need for further refinement or exploring alternative methods to improve performance in this area.

- The comparison between traditional Machine Learning models and Deep Learning techniques was limited to this study's specific models and approaches, potentially excluding other models that may demonstrate enhanced performance.

8.2 Next steps

- Expand the dataset to include more diverse samples, allowing for more robust testing and generalizability of the results.

- Test other segmentations (i.e., red blood cells) and combine them to remove biases due to white balance or color tinting.

- Our results indicate that benign cells are often hard to differentiate from early-stage cells. Having a dataset with more healthy controls could improve our accuracy.

- Investigate and implement additional feature extraction and classification techniques to enhance cancerous and non-cancerous cell classification accuracy. Specifically, increased segmentation accuracy would allow for Nucleus to Cytoplasm “N/C” ratio feature, which would be an important feature given the research papers explored in the literature review.

- Explore the potential of integrating CNNs and SVMs in a hybrid model to capitalize on the strengths of both methods and improve overall performance.

- New models are frequently being created and updated. These tests will have to be further repeated as new SOTA techniques emerge.

- Extend the research scope to other types of cancer and related diagnostic procedures, broadening the applicability and utility of the developed methods.

9. References

1. Leukemia and Lymphoma Society. (2021). Facts and Statistics. https://www.lls.org/facts-and-statistics/facts-and-statistics-overview
2. American Cancer Society. (2018, October 17). Tests for Acute Lymphocytic Leukemia (ALL). https://www.cancer.org/cancer/acute-lymphocytic-leukemia/detection-diagnosis-staging/how-diagnosed.html
3. Wenbin He, Ting Liu, Yongjie Han, Wuyi Ming, Jinguang Du, Yinxia Liu, Yuan Yang, Leijie Wang, Zhiwen Jiang, Yongqiang Wang, Jie Yuan, & Chen Cao. A review: The detection of cancer cells in histopathology based on machine vision. Computers in Biology and Medicine, Volume 146, 2022, 105636. https://doi.org/10.1016/j.compbiomed.2022.105636.
4. Luis H.S. Vogado, Rodrigo M.S. Veras, Flavio. H.D. Araujo, Romuere R.V. Silva, Kelson R.T. Aires. Leukemia diagnosis in blood slides using transfer learning in CNNs and SVM for classification. Engineering Applications of Artificial Intelligence, Volume 72, 2018, Pages 415-422, ISSN 0952-1976. https://doi.org/10.1016/j.engappai.2018.04.024.
5. Sahlol, A.T., Kollmannsberger, P. & Ewees, A.A. Efficient Classification of White Blood Cell Leukemia with Improved Swarm Optimization of Deep Features. Sci Rep 10, 2536 (2020). https://doi.org/10.1038/s41598-020-59215-9
6. Abd El-Ghany S, Elmogy M, El-Aziz A. Computer-Aided Diagnosis System for Blood Diseases Using EfficientNet-B3 Based on a Dynamic Learning Algorithm. Diagnostics (Basel). 2023 Jan 22;13(3):404. doi: 10.3390/diagnostics13030404. PMID: 36766509; PMCID: PMC9913935.
7. Hegde RB, Prasad K, Hebbar H, Singh BMK, Sandhya I. Automated Decision Support System for Detection of Leukemia from Peripheral Blood Smear Images. J Digit Imaging. 2020 Apr;33(2):361-374. doi: 10.1007/s10278-019-00288-y. PMID: 31728805; PMCID: PMC7165227. https://www.ncbi.nlm.nih.gov/pmc/articles/PMC7165227/
8. Mehrad Aria, Mustafa Ghaderzadeh, Davood Bashash, Hassan Abolghasemi, Farkhondeh Asadi, and Azamossadat Hosseini, “Acute Lymphoblastic Leukemia (ALL) image dataset.” Kaggle, (2021). DOI: 10.34740/KAGGLE/DSV/2175623.
9. Das, P.K., Jadoun, P., & Meher, S. (2020). Detection and Classification of Acute Lymphocytic Leukemia. 2020 IEEE-HYDCON, 1-5.
10. Nimesh Patel, Ashutosh Mishra. Automated Leukaemia Detection Using Microscopic Images, Procedia Computer Science, Volume 58, 2015, Pages 635-642, ISSN 1877-0509 https://doi.org/10.1016/j.procs.2015.08.082.
11. V. Singhal and P. Singh, "Local Binary Pattern for automatic detection of Acute Lymphoblastic Leukemia," 2014 Twentieth National Conference on Communications (NCC), Kanpur, India, 2014, pp. 1-5, doi: 10.1109/NCC.2014.6811261.
12. Saba Saleem, Javaria Amin, Muhammad Sharif, Ghulam Ali Mallah, Seifedine Kadry, and Amir H. Gandomi, Leukemia segmentation and classification: A comprehensive survey, Computers in Biology and Medicine, Volume 150, 2022, 106028, ISSN 0010-4825, https://doi.org/10.1016/j.compbiomed.2022.106028. (https://www.sciencedirect.com/science/article/pii/S001048252200748X)
13. Acharya V, Kumar P. Detection of acute lymphoblastic leukemia using image segmentation and data mining algorithms. Med Biol Eng Comput. 2019 Aug;57(8):1783-1811. doi: 10.1007/s11517-019-01984-1. Epub 2019 Jun 14. PMID: 31201595.
14. Eddins, S. (2013, November 19). *Watershed transform question from Tech Support*. Steve on Image Processing with MATLAB. Retrieved April 22, 2023, from https://blogs.mathworks.com/steve/2013/11/19/watershed-transform-question-from-tech-support/
15. Mingxing Tan and Quoc V. Le, “EfficientNetV2: Smaller Models and Faster Training,” (2021) (https://doi.org/10.48550/arXiv.2104.00298)
16. Morteza Moradi Amin, Saeed Kermani, Ardeshir Talebi, and Mostafa Ghelich Oghli, Recognition of Acute Lymphoblastic Leukemia Cells in Microscopic Images Using K-Means Clustering and Support Vector Machine Classifier (2015) (https://www.ncbi.nlm.nih.gov/pmc/articles/PMC4335145/)
17. Thukral, S., Meisheri, H., Kataria, T., Agarwal, A., Verma, I., Chatterjee, A., & Dey, L. (2018, August). Analyzing behavioral trends in community driven discussion platforms like reddit. In *2018 IEEE/ACM International Conference on Advances in Social Networks Analysis and Mining (ASONAM)* (pp. 662-669). IEEE.